

Energy Savings for Gas Preheating in the Gas Transport Sector with Air Dehumidification and Expansion Turbines

Lisa Völker¹, Yoann Louvet¹, Daniel Fleig¹, Felix Pag¹, Ulrike Jordan¹, Klaus Vajen¹

¹ University of Kassel, Institute of Thermal Engineering, Kassel (Germany)

Abstract

In gas pressure regulating and metering stations (GPRMS) natural gas is reduced from high pressure to almost atmospheric pressure for the end consumer. To avoid, among others, freezing of pipelines and other components which the natural gas passes through, the gas is preheated before the throttling process. This work presents two different technologies with the objective to reduce the primary energy demand for the preheating of the natural gas: the dehumidification of the air of the gas expansion room and the combination of an expansion turbine with electrical heat pumps. The energy savings regarding the air dehumidification of a GPRMS could be evaluated based on measured data. A long-term field test with a novel liquid desiccant air conditioning system was carried out and based on the measured data the primary energy demand of the studied GPRMS could be reduced about 12 % for the year 2021 compared to a reference case without dehumidification. First theoretical investigations reveal that by designing the expansion turbine and heat pump unit to cover the total typical heat demand of the studied GPRMS in summer, 90 % primary energy savings can be achieved on typical summer days, 39 % in autumn / spring and 19 % in winter, considering the total energy consumption of the GPRMS (electric power and heat demand).

Keywords: gas pressure regulating and metering station, energy efficiency, liquid desiccant, dehumidification, expansion turbine

1. Introduction

Gas pressure regulating and metering stations (GPRMS) are important facilities in natural gas distribution networks, in which the gas pressure is reduced from the high pressure required to transport it over long distances to almost atmospheric pressure for the end consumers. GPRMS are an equivalent to transformer stations in the electric grid. In GPRMS the natural gas is usually throttled, leading to a temperature decrease of the gas of between 0.4 and 0.7 K/bar, depending on its composition and the operating conditions (Mischner et al., 2015). In Germany, in order to avoid freezing in the GPRMS and downstream pipelines after the throttling process, it is state of the art to preheat the natural gas with gas boilers. The energy requirement for preheating depends on the natural gas mass flow through the station, which is driven by demand and on the physical properties of the gas. In total, all German GPRMS consume about 2 TWh/a primary energy for natural gas preheating (Mischner et al., 2019).

An analysis of existing heating systems in GPRMS shows that several efficiency measures can usually be taken to reduce the energy consumption for preheating. Optimised control strategies and adapted hydraulic concepts can, for example, reduce the heat demand and further lower the flow temperature level required for preheating, usually to between 40 and 80 °C. This favours the integration of energy efficient heat supply technologies in a second step. In previous studies by Wimmer et al. (2019) and Louvet et al. (2021) several strategies are presented that include the combination of innovative technologies, which have been applied at several GPRMS in Germany to reduce their primary energy consumption. Two additional innovative technologies, not investigated so far and aiming at further reducing the primary energy consumption of GPRMS, are presented in this work. These are the dehumidification of the room where the gas expansion takes place (gas expansion room) and the combination of expansion turbine and heat pumps. Regarding the energy saving potential due to dehumidification a long-term field test was carried out at an existing commercial GPRMS and measurement data are analysed whereas for the latter presented investigations and results are based on theoretical calculations in this paper.

2. Studied GPRMS

Both GPRMS which are the focus of the present study are installed in Central Germany and are already equipped with solar heat for industrial processes (SHIP) plants and with gas absorption heat pumps (GAHPs) in addition to

conventional gas boilers for the preheating of the natural gas.



Fig. 1: Pictures of the GPRMS Ostheim with a 295 kW_{th} SHIP plant and 123 kW_{th} GAHP (left) and the GPRMS Neu-Eichenberg with a 95 kW_{th} SHIP plant and 123 kW_{th} GAHP (right).

The GPRMS Ostheim (Fig. 1, left) has a useful heat demand more than twice as large as the GPRMS Neu-Eichenberg (Fig. 1, right). The shares of the total useful heat demand covered by the different technologies are summarised in Tab. 1. Primary energy savings of 36 % (GPRMS Ostheim) and 33 % (GPRMS Neu-Eichenberg) are achieved with the existing innovative technologies in comparison to a calculated reference scenario, in which the energy for preheating is supplied only with gas boilers. In addition, the downstream gas temperature is assumed to be constant throughout the year at 10 °C in the reference scenario, whereas both stations are equipped with a dew point control of the downstream gas temperature, also contributing to the total primary energy savings indicated.

Tab. 1: Useful heat demand and share covered by the different heating technologies for the studied GPRMS

GPRMS	Useful heat demand in MWh/a	Share gas boiler in %/a	Share GAHPs in %/a	Share SHIP plant in %/a
Ostheim	1,450	57	29	14
Neu-Eichenberg	690	43	50	7

The approximation method for calculating the heat capacity for preheating the natural gas $\dot{Q}_{phys,PH}$ to compensate the gas temperature reduction is specified by the DVGW regulations G 499 (DVGW, 2015) according to equation 1.

$$\dot{Q}_{phys,PH} = \dot{V}_n \cdot \rho_n \cdot c_{p,m} \cdot (\mu_{JT,m} \cdot (p_u - p_d) + T_d - T_u) \quad (1)$$

In addition to the natural gas volume flow \dot{V}_n in the standard state ($T_n = 273,15$ K und $p_n = 1013,25$ mbar), the heating capacity depends on the composition of the natural gas as well as the pressure and temperature before heating (p_u, T_u) and after expansion (p_d, T_d). The natural gas inlet temperature T_u approaches the ground temperature. The gas outlet temperature T_d (GOT) is the decisive variable to be controlled to reduce the heat demand for gas preheating. Since the actual heat consumption in a GPRMS is higher due to system and heat losses, the one calculated according to equation (1) is also referred to as the physical heat demand and represents a theoretical value.

3. Dehumidification of GPRMS with liquid desiccant air conditioning (LDAC) system

To avoid condensation on the pipe surfaces after expansion of the natural gas a dew point controller can be implemented. This ensures that the natural gas outlet temperature (GOT) is always a defined temperature difference higher than the dew point temperature of the gas expansion room. The energy demand for preheating the natural gas can be further reduced by dehumidification of the room air. Assuming a minimal allowable GOT of 4 °C and a temperature difference of 3 K for the dew point control the dew point temperature of the gas expansion room should be at least 1°C which corresponds to a humidity ratio of air of 4.5 g/kg. Conventional dehumidifier working with dew point cooling cannot be operated economically at this level of humidity anymore, because icing of the cooling coil leads to energy consuming defrosting. Another way of dehumidification uses sorption processes, either adsorption (with desiccant wheels) or absorption processes. The latter are realized in liquid desiccant air conditioning (LDAC) systems, considered in the present research.

3.1. Operating principle of LDAC system and integration to GPRMS

Fig. 2 (a) shows the operating principle of such a system which consists mainly of two heat and mass exchangers –

the absorber (conditioner) and the regenerator –, a solution-to-solution heat exchanger and a solution tank. The hygroscopic solution (LiCl-H₂O) gets into direct contact with the outdoor air (OA) in the dehumidifier. Because of the difference in water vapor partial pressure between the ambient air and above the solution surface, water molecules of the air are absorbed by the solution and the air is dehumidified. During the absorption process heat is released. In the LDAC system investigated in this project, the absorber can be cooled internally by a pipe coil through which water flows. Compared to systems without internal cooling, this offers the advantage that the heat released during absorption can be removed by the cooling water which improves the dehumidification efficiency. However, operation without cooling water (adiabatic mode) is also possible for the used LDAC system. After the absorption process the diluted solution is concentrated again in the regenerator. For that process heat is required on a temperature level of 50 to 80 °C depending on the needed dehumidification. The cooling water is provided by a wet-cooling tower and the heat for the regeneration process is provided by a solar thermal plant and gas absorption heat pumps as mentioned before. LDAC systems like the described one have so far only been used in a few pilot systems in Europe.

An LDAC system was implemented at GPRMS Neu-Eichenberg in 2020 (see Fig. 2 (b)) and has been monitored since then in a long-term test. For GPRMs state of the art is that the fresh air supply for the gas expansion room is realized by natural ventilation with louvre in the wall. For the field test mechanical ventilation was implemented to supply the dehumidified fresh air to the gas expansion room.

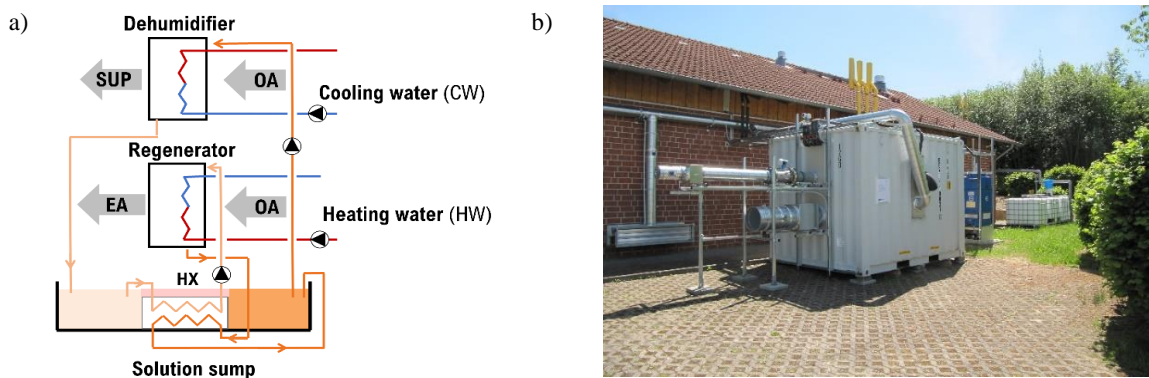


Fig. 2: (a) Operating principle of LDAC system and (b) LDAC system in a maritime container in front of GPRMS Neu-Eichenberg

3.2. Method

In order to determine the reached yearly energy savings through dehumidification, the physical heat demand is first determined according to equation 1 using the measurement data from the gas network operator ($Q_{phys,meas}$) for the year 2021. For the reference case, the physical heat demand must also be determined in the event that no air dehumidification takes place ($Q_{phys,ref}$). For this reference case, it is assumed that the humidity ratio in the gas expansion room corresponds to that of the outside air (natural ventilation). Thus, the dew point temperature in the room and also the GAT can be determined for the reference case. In 2021, the offset from the measured dew point temperature in the gas expansion room to the GOT was 5 K until July and 3 K from August. The same offset is also assumed for the reference case. Since heat (Q_{reg}) is required for the regeneration process, this must be taken into account when determining the savings, so that the heat saved (Q_{save}) based on the calculation of the physical heat demand, can be calculated according to equation 2.

$$Q_{save} = Q_{phys,PH,ref} - Q_{phys,PH,meas} + Q_{reg} \quad (2)$$

Based on measurement data for the to be depressurized natural gas and the heating gas consumption for the year 2017-2019 the average ratio of energy supplied by fossil fuel (heating gas) to calculated physical heat demand is 1.15. Assuming that value also for the reference case without dehumidification the heating gas consumption (for the boiler and GAHPs) can be estimated. Thus, besides the savings based on the theoretical physical heat demand also the primary energy savings can be determined. Therefore also the electrical power consumption of the LDAC system is considered with primary energy factor for electricity of 1.8.

It turned out, that the deviation of the measurement data for the relative humidity of the air at the absorber inlet is outside the measurement uncertainties of the sensors. The relative humidity (RH) is used to calculate the dew point

temperature for the reference case without dehumidification. In order to be able to estimate the savings in preheating despite the measurement deviation, a correction curve was determined by calibrating the sensors, which was applied to the measurement data for 2021. For areas that the correction curve cannot depict ($RH > 90\%$), data from a nearby weather station are used. In addition, the measurement data for the pressure of the natural gas before expansion and the measurement data for the gas outlet temperature (in minute time steps) are missing for August 2021. Since the gas pressures remained almost constant over the entire considered period, the inlet pressure for August is assumed to be 50 bar and hourly measured values were used for the GOT.

3.3. Measurement data and results

The measured volume flow rate at standard conditions for the to be depressurized natural gas is shown in Fig. 3 for the year 2021. The total gas volume for the year 2021 was $80.7 \cdot 10^6 \text{ Nm}^3$. The mean daily upstream pressure in 2021 was 51 bar and the mean daily downstream pressure was 14.4 bar in summer and 8 bar in winter. Fig. 4 shows the measured humidity ratio of the air at the absorber inlet $\omega_{abs,in}$ and absorber outlet $\omega_{abs,out}$ as well as the necessary humidity ratio to reach the minimal GOT of 4°C (ω_{goal}) for the year 2021. Also in the winter months there is a need for dehumidification on some days, since the humidity ratio of the air is above ω_{goal} . In July 2021 the temperature difference (between the GOT and the dew point temperature of the air) of the dew point control was reduced from 5 K to 3 K which results in an increase of ω_{goal} .

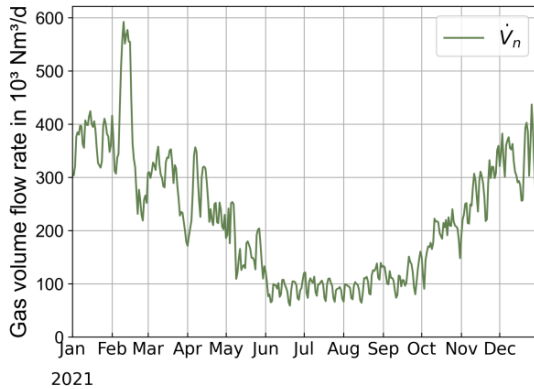


Fig. 3: Measured volume flow rate at standard conditions of the to be depressurized natural gas for the year 2021

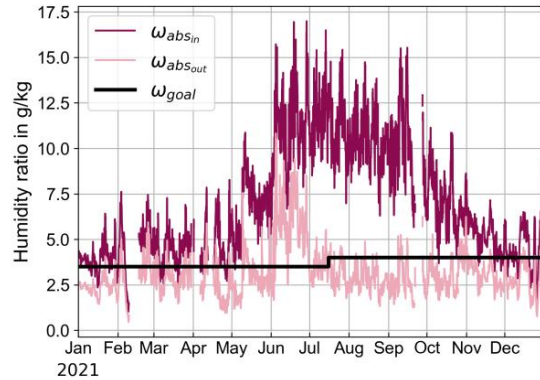


Fig. 4: Measured humidity ratio at absorber inlet $\omega_{abs,in}$ and outlet $\omega_{abs,out}$

The wet cooling tower to provide the cooling water for the absorber was put into operation in April 2021. During the year 2020 the LDAC system was operated adiabatic (without cooling of the absorber). The evaluation of the measurement data show that the dehumidification is more effective with internal cooling as shown in Fig. 5. The mean hourly humidity ratio difference $\Delta\omega$ of inlet and outlet humidity ratio depending on the inlet humidity ratio at the absorber is plotted for the operation of the LDAC system with and without internal cooling (adiabatic) for the years 2020 and 2021. Especially in summer for higher outdoor air humidity ratios the humidity ratio difference $\Delta\omega$ can be more nearly doubled if the absorber of the LDAC system is cooled by the wet cooling tower and heat supply to the regenerator is sufficient. Taking as example an inlet air humidity ratio of 13 g/kg an average humidity ratio difference of 5 g/kg and 9.4 g/kg is reached in adiabatic operation and with internal cooling respectively.

The results of the dehumidification regarding the GOT for the year 2021 are shown in Fig. 6. The measured GOT with dehumidification ($T_{d,meas}$) and a calculated GOT without dehumidification ($T_{d,ref}$) assuming that the dew point temperature of the gas expansion room is equal to that of the ambient air (due to natural ventilation) are plotted. Due to the dehumidification, the minimum GOT of 4°C is reached in about 80% of the operating hours. In total, the GOT of 4°C was exceeded for 1,800 hours, of which approx. 750 hours can be traced back to June and September, when the LDAC system ran faulty or was completely out of order. In June the major problem was the heat supply for the regeneration so that the mean hot water inlet temperature at the regenerator was only 38°C whereas it was 58°C for the remaining summer month. Due to the lower hot water temperatures in June the dehumidification is clearly restrained. As mentioned before the hot water for the regeneration is supplied by the GAHPs and the solar thermal plant and for that reason is somehow restricted. By the dehumidification the GOT could be reduced by an average of 12 K in summer and 2 K in winter month.

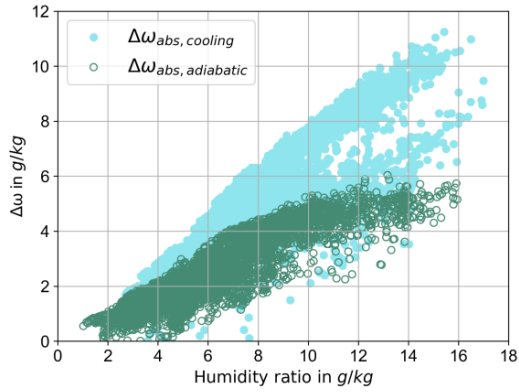


Fig. 5: Mean hourly humidity ratio difference $\Delta\omega$ of inlet and outlet humidity ratio depending on the inlet humidity ratio at the absorber for the operation of the LDAC system with and without internal cooling (adiabatic) for the years 2020 and 2021

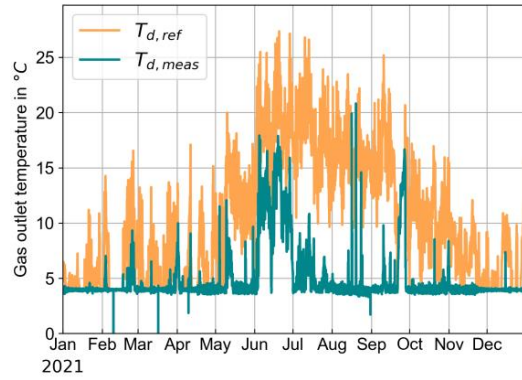


Fig. 6: Measured GOT with dehumidification (T_{meas}) and theoretical GOT without dehumidification (T_{ref}) for the year 2021

Based on the given GOT the physical heat demand for the measured data $Q_{phys,meas}$ and the reference case $Q_{phys,ref}$ is calculated and shown in Fig. 7. Besides the physical head demand also the measured heat for the regeneration Q_{reg} is considered. The physical heat demand $Q_{phys,meas}$ amounts to a total of 608 MWh and the heat consumption for the regeneration Q_{reg} to 40.5 MWh for 2021. If a GOT of 4 °C had been realized the whole year the physical heat demand would have been 589 MWh which corresponds to the maximal energy saving potential. This means the maximal potential regarding only the physical heat demand was missed by 3.2 %.

The physical heat demand $Q_{phys,ref}$ for the reference case without dehumidification is 747 MWh. As expected, the savings regarding the physical heat demand are highest in the summer months when outdoor air humidity ratio is high as shown in Fig. 8. The faulty operation of the LDAC system due to problems with hot water supply are clearly noticeable for the month June. Further although the natural gas volume flow rate is the lowest during summer month, highest savings can be determined during that time. However, this also requires the highest heat consumption for the regeneration (see Fig. 7). In 2021, the heat demand was reduced by a total of 99 MWh taking into account the regeneration heat, compared to the reference case thanks to the dehumidification of the gas expansion room air. This corresponds to a reduction of 13.2 %. Without the failure of the heat supply in June and the shutdown of the LDAC system in September, the reduction would have been even higher. In addition to the required regeneration heat, however, the power consumption for the LDAC system must also be taken into account. In 2021, this amounts to 3 MWh for the LDAC system.

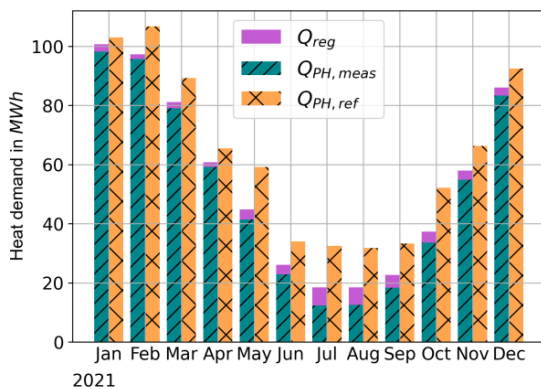


Fig. 7: Monthly physical preheating demand for the measured data $Q_{phys,PH,meas}$ and the reference case without dehumidification $Q_{phys,PH,ref}$ as well as the measured heat demand for the regeneration Q_{reg} for the year 2021

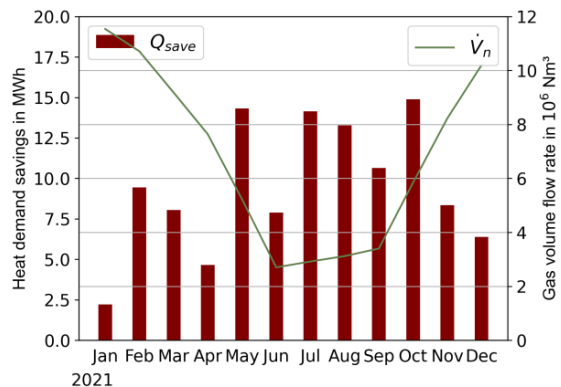


Fig. 8: Calculated monthly savings Q_{save} in physical heat demand based on measured data compared to reference case without dehumidification and natural gas volume flow rate at standard conditions for the year 2021

The heating gas consumption for the GAHPs and the gas boiler was 74,160.3 Nm³ in 2021 which corresponds to a total heat input by fossil fuels of 754 MWh. It should be considered that from the middle of November until the end of the year 2021 the regenerative heat supply (GAHPs and ST) was not in operation. During that time only the gas boilers covered the preheat demand which led to higher heating gas consumption during that month compared to other years. The primary energy input including the electricity consumption for the LDAC system is 834.8 MWh. Assuming a ratio of 1.15 of physical heat demand to heat input by fossil fuels the primary energy input for the reference case is 945 MWh. Based on this assumption the primary energy could be reduced by 11.6 % for the year 2021.

4. Combination of expansion turbine and heat pumps

During the throttling process, the potential energy contained in the gas at high pressure is not used. Alternatively, the gas can be expanded in an expansion turbine to generate electricity. It is reported that in Germany expansion turbines with a total capacity of 70 MW_{el} are already installed at GPRMS (Mischner et al., 2015). However, the installed turbines are in the range of several 100 kW_{el}, which limits their scope of application to the largest GPRMS with a high gas throughput. A research project was initiated aiming at developing a smaller turbine in the range of a few tens of kilowatts and at demonstrating its application in combination with electric heat pumps, with the aim of supplying the energy demand for gas preheating of the GPRMS.

The pressures indicated in this chapter are absolute pressures. The calculations are performed with the programming language Python, notably using the library NeqSim (Solbraa, 2022) for the determination of the physical properties of the gases considered.

4.1. The natural gas expansion process

The gas expansion process in an expansion turbine is presented in Fig. 9. The gas states before and after the expansion turbine (Fig. 9, left) are represented in a (h-s) diagram in Fig. 9 (right). The ideal expansion, between the points *u,ex* and *ds,ex* is isentropic. The corresponding change in enthalpy Δh_s expresses the theoretical work that can be transferred outside of the system. The work actually transferred from the gas stream to the turbine wheel is characterised by the isentropic efficiency η_s of the expansion turbine. For the considered application isentropic efficiencies between 0.6 and 0.7 can be expected.

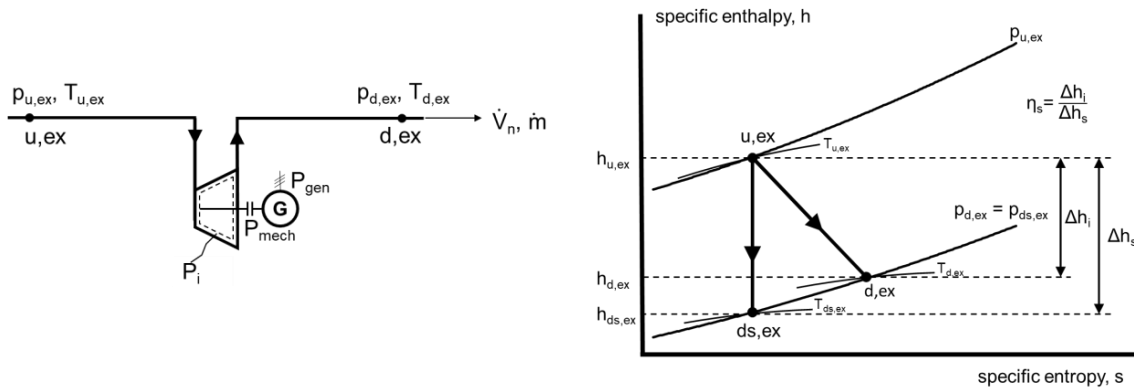


Fig. 9: Hydraulic scheme of an expansion turbine in a gas pipeline (left) and representation of the expansion process in a (h-s) diagram (right) adapted from Mischner et al. (2015)

An impulse turbine is the chosen technology to achieve the gas expansion. With this type of expansion turbine the gas pressure reduction (from $p_{u,ex}$ to $p_{d,ex}$) takes place exclusively in the nozzle situated before the turbine wheel and results in an increase of the gas kinetic energy, which is maximal at the nozzle outlet. For converging nozzles, the gas velocity at the nozzle outlet is limited by the sound velocity. This implies that for a given nozzle exit (throat) area the maximum possible gas flow rate is achieved when the gas reaches sonic velocity. This state corresponds to the so-called critical condition for operating the nozzle. In a nozzle, pressures and velocity are linked. The critical velocity therefore corresponds to a given pressure ratio between the downstream and upstream pressures of the nozzle, which depends on the gas composition and the operating conditions (gas pressures and temperatures). For methane for instance, in the temperature and pressure ranges relevant for GPRMS, the pressure ratio varies between 0.50 and 0.55. As an example for $p_{u,ex} = 40$ bar, critical velocity is reached for $p_{d,ex} = 21$ bar. In this condition the pressure reached downstream is called the critical pressure and is usually referred to as p^* . It is possible to further

reduce the pressure at the nozzle (i.e. expansion turbine) outlet below p^* and operate the expansion turbine in supercritical conditions. In this case the gas experiences a post-expansion at the nozzle outlet from p^* to the expansion turbine downstream pressure (lower than p^*). Another solution consists in using a converging-diverging nozzle, also called de Laval nozzle. In this configuration supersonic gas velocities can be achieved at the outlet of the nozzle.

The flow in the nozzle is almost isentropic, which means that the gas temperature at the outlet of the nozzle is close to $T_{ds,ex}$. Considering methane, for an upstream pressure of 40 bar, a pressure ratio of 0.5, $\eta_s = 0.6$ and $T_{d,ex} = 5^\circ\text{C}$ the calculated $T_{ds,ex}$ amounts to -10.3°C . It remains to be clarified if this local, between nozzle outlet and turbine wheel, low gas temperature could be a problem for the operation of the turbine. One option to avoid low temperatures at the nozzle outlet is to increase the downstream gas temperature $T_{d,ex}$, which would result in an almost equivalent increase in $T_{ds,ex}$. However, this is not optimal from an energetic point of view, as it also corresponds to an almost equivalent increase in $T_{u,ex}$.

4.2. Integration of the expansion turbine combined with a heat pump in an existing GPRMS

Keeping the required upstream gas temperature of the turbine $T_{u,ex}$ to the lowest level possible is indeed crucial, as the main idea of the project consists in using heat pumps in combination with the expansion turbine to provide the requested energy to preheat the gas. The heat pump should use the ambient air as heat source and should be driven by the expansion turbine. A hydraulic scheme of the integration of an expansion turbine combined to an electric heat pump in an existing GPRMS is presented in Fig. 10. The existing installation in grey consists of two redundant parallel gas lines. More information about the function of the different components can be found in Wimmer et al. (2019) and Louvet et al. (2021) for instance. The expansion turbine is connected in parallel to the existing pressure reduction lines and aims at reducing the pressure of part of the gas flow circulating through the station. The pressure of the remaining gas flow being reduced with a gas pressure regulator in the existing gas lines. The components required to integrate the expansion turbine are indicated in green in the block marked T-U (expansion turbine unit). It consists in different valves and safety devices as well as an additional gas preheater, as the required upstream gas temperature of the expansion turbine is higher than the one required before the gas pressure regulator. Also, an additional gas pressure regulator might be required in the expansion turbine unit (not represented) if the design pressure ratio of the expansion turbine is higher than the ratio between downstream and upstream GPRMS pressures. The combination of the expansion turbine, the heat pump and the related components is marked T-HP-U (expansion turbine and heat pump unit).

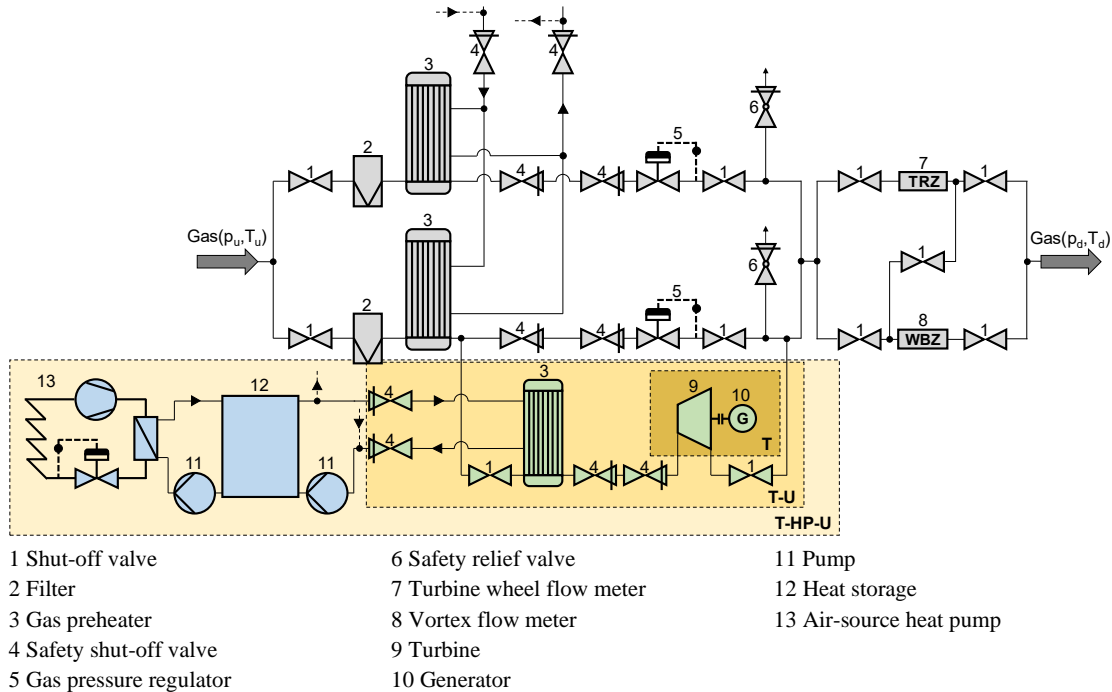


Fig. 10: Hydraulic scheme of the integration of an expansion turbine combined to a heat pump in an existing GPRMS

Dimensioning the expansion turbine is a complex task, depending on several technical, economic and regulatory parameters. To illustrate part of the challenges, measurement data from the GPRMS Ostheim are shown for the year 2020 in Fig. 11 with a daily resolution. The gas volume flow rate (Fig. 11, left) varies greatly along the year due to the seasonality of the gas demand. There is a factor eight between the mean daily gas volume flow rate in the summer

months and the peak volume flow rate at the end of January. There is thus a first compromise to make between reaching a high number of full load hours (FLH) for the expansion turbine and heat pump unit corresponding to an economic optimum and minimising the CO₂ emissions of the GPRMS. The higher the nominal gas flow rate the expansion turbine and heat pump unit is designed for, the less remaining heat demand for gas preheating the auxiliary gas boiler needs to cover, but the lower the number of FLH of the unit. The pressure levels at the GPRMS (Fig. 11, right) also play an important role in the design of the expansion turbine as mentioned in section 4.1. The mean daily upstream pressure experiences important variations along the year of 26.6 bar between its minimum and its maximum. On the opposite the mean daily downstream pressure is set to a constant value. Two different operating levels of 15.5 bar in the winter and 10.8 bar in the summer (between mid-April and beginning of October) can be identified.

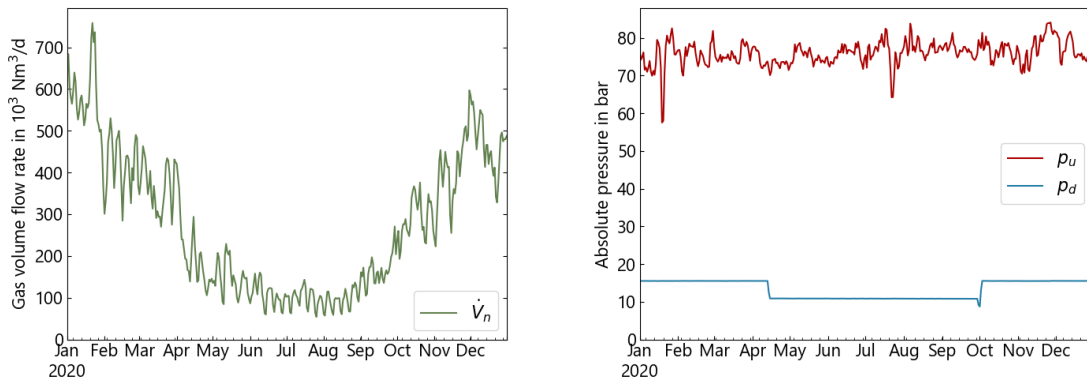


Fig. 11: Measured daily gas flow rate (left) and mean daily pressure levels (right) at the GPRMS Ostheim for the year 2020

Varying pressure conditions are a challenge as the expansion turbine (nozzle, turbine wheel) is designed for given pressure levels. Deviating from the nominal parameters, not only pressures but also flow rate, results in a decrease of the efficiency of the expansion turbine, and thus a lower power output at the generator. The varying upstream pressure is not a relevant issue for the considered GPRMS, as the total pressure reduction is anyway too important to be achieved solely by the expansion turbine. This is illustrated in Fig. 12, representing the calculated required gas temperature upstream of the expansion turbine (red dots) depending on the upstream pressure for a set downstream pressure of 12 bar as well as set downstream temperatures of 5 °C (Fig. 12, left) and 15 °C (Fig. 12, right) for methane. The isentropic efficiency of the expansion turbine is set to 0.65. The evolution of the upstream gas temperature required for the expansion process with the turbine follows a logarithmic pattern. With the considered assumptions, reducing the gas pressure from 58 to 12 bar with the expansion turbine requires an upstream gas temperature of 83 °C. Assuming a logarithmic mean temperature difference (LMTD) of 10 K at the gas preheater and considering distribution losses, this would require the heat pump to supply a flow temperature of at least 95 °C, outside the range of what air-source heat pumps can deliver. For the GPRMS Ostheim it is therefore necessary to reduce the upstream gas pressure before the expansion turbine to an acceptable level. The observed variations of the gas upstream pressure are thus not a problem for the design of the expansion turbine as far as the nominal upstream pressure is not higher than the minimum supply upstream pressure of the GPRMS. This minimum upstream pressure is usually contractually defined between the operator of the GPRMS and the upstream gas network operator.

For comparison purposes the required upstream gas temperature for the same pressure reductions but achieved with a gas pressure regulator (throttling) is also represented (blue dots) in Fig. 12. The upstream gas temperature required for the throttling increases almost linearly with the upstream pressure at a rate of 0.4 to 0.5 K/bar in the ranges considered. Compared to the expansion process, the required upstream gas temperature and therefore the required energy for preheating is significantly lower for the throttling.

The comparison of both downstream gas temperature levels (Fig. 12 left and right) also shows that an increased downstream gas set temperature, for instance in summer to avoid water vapour condensation on the outer surface of downstream pipes, correspond to an equivalent increase in the required upstream gas temperature. With an upstream gas pressure of 58 bar, the increase of 10 K of the downstream gas set temperature requires an increase of 10.9 K of the upstream gas temperature.

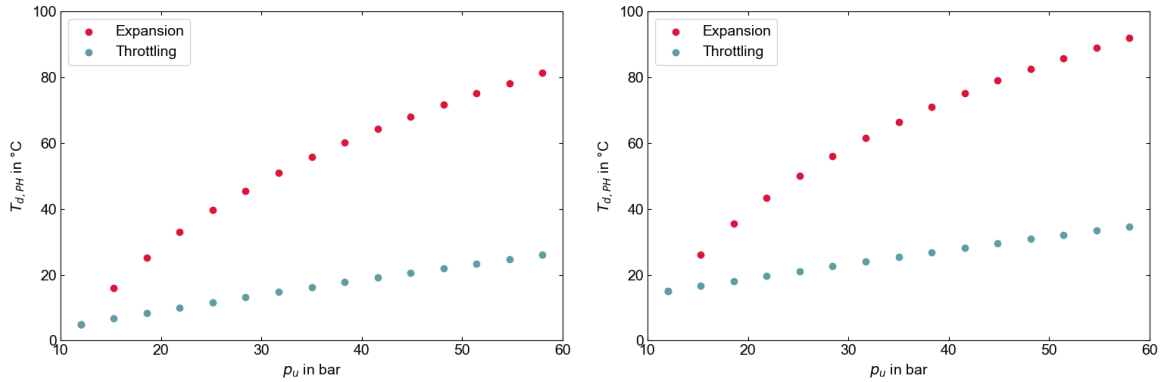


Fig. 12: Calculated upstream gas temperatures for different upstream gas pressures for an expansion process and a throttling process. Calculated for methane with a fixed downstream pressure $p_d = 12$ bar and a fixed downstream temperature $T_d = 5$ °C (left) and $T_d = 15$ °C (right). For the expansion process the isentropic efficiency is fixed, $\eta_s = 0.65$.

The variations of the gas downstream pressure (Fig. 11, right) are more problematic for the design of the expansion turbine. Several options can be considered. One consists in designing the expansion turbine for a downstream pressure situated in-between the pressure levels in summer and in winter, so that the expansion turbine never operates in nominal conditions, but the operating point is never “too far” from the design point. The installation of an additional gas pressure regulator downstream of the expansion turbine is another option, linked to increased investment costs and more space requirements. At network level, keeping a constant downstream pressure throughout the year could be also considered, if the operation of downstream GPRMS allows it.

The rated capacity of the power line connecting the GPRMS to the grid is also an important parameter to consider for the design of the expansion turbine. GPRMS are usually situated outside inhabited areas, thus far from main power lines, so that an extension of the rated capacity of the connecting line is often not an option due to the high related costs. The capacity of the line might then be a limiting factor when the expansion turbine additionally to covering the needs of the heat pump is designed to cover the power needs of the GPRMS and export surpluses to the grid. Even if attractive on paper, connecting the expansion turbine to the grid also comes with complications. Indeed, only small network operators as defined by the regulator (BMJV, 2021) are allowed to supply power to the grid due to EU rules on unbundling in the energy sector. According to the current legislation, larger network operators would have to delegate the operation of the expansion turbine to a contractor if they aim at supplying power surpluses to the grid.

4.3. Energetic comparison between throttling process and expansion process

A comparison of the energy flows between the conventional throttling process and the process including an expansion turbine combined to a heat pump is presented in Fig. 13 for identical upstream and downstream conditions.

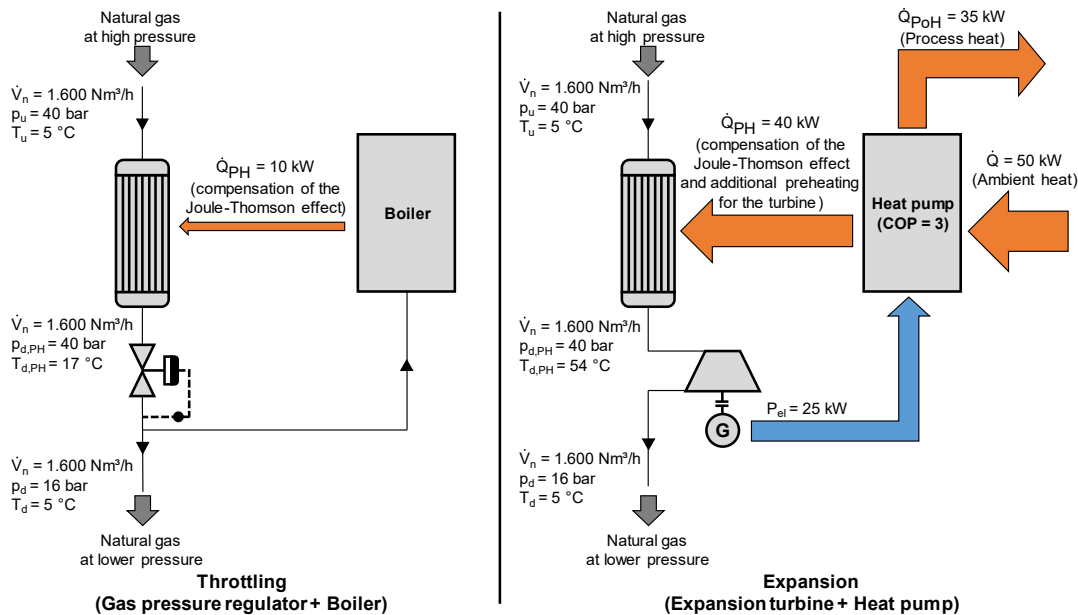


Fig. 13: Schematic comparison of the energy flows in the throttling process (left) and in the process including the expansion turbine (right)

As mentioned in section 4.2 the required gas temperature $T_{d,PH}$ at the outlet of the gas preheater is significantly higher before the expansion turbine than before the gas pressure regulator. In the presented case the heating power needed to preheat the gas is four times higher when using the expansion turbine. Also, the expansion turbine is designed to supply the heat pump exclusively. With an assumed coefficient of performance (COP) of 3, 53 % of the heat output of the heat pump is used to preheat the gas before the expansion turbine, while the remaining 47 % (\dot{Q}_{PoH}) can be used to preheat the rest of the natural gas flowing through the GPRMS, for which the pressure is reduced with a conventional throttling process instead of using an expansion turbine.

To theoretically compare the conventional throttling process with the expansion process from an energetic point of view, the GPRMS Ostheim in 2020 is taken as case study (see Fig. 11). For the integration of the expansion turbine unit, the hydraulic configuration presented in Fig. 14 is considered. All the gas flowing through the station is preheated in a first gas preheater, to a temperature allowing to reach the set GOT (T_d) after throttling. Part of the total gas stream flowing through the station flows through the expansion turbine unit while the rest of the gas stream passes through the existing line with the conventional gas pressure regulator. The gas stream flowing through the expansion turbine unit requires a pre-throttling and an additional preheating before passing through the expansion turbine for the reasons explained in section 4.2.

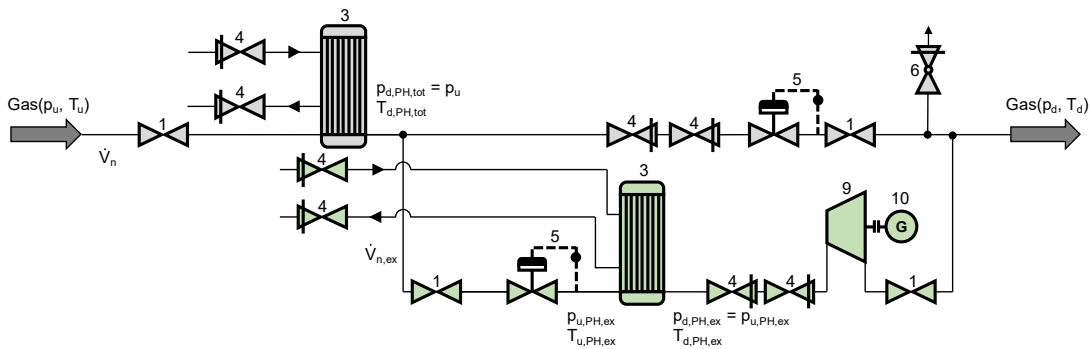


Fig. 14: hydraulic scheme of the considered integration of the expansion turbine unit at the GPRMS Ostheim. The description of the components is given in Fig. 10.

Three operating conditions are compared, corresponding to average operating conditions at the GPRMS Ostheim in summer (mean from June to August), winter (mean from December to February) and autumn / spring (mean from September to November and March to Mai). The temperatures and gas flow rate are averaged over these periods. The measured upstream gas temperature follows the ground temperature at a depth of 1.5 m and the set GOT varies along the year and follows the dew point of the ambient air to avoid condensation on the outside of downstream pipes and components. For simplification purposes the upstream and downstream pressures are considered constant over the year at 76 bar, respectively 14.5 bar corresponding to the flow rate-weighted averages.

The expansion turbine and heat pump unit are designed to cover the entire heat demand of the station for gas preheating on average summer operating conditions. The upstream pressure of the expansion turbine $p_{d,PH,ex}$ is set to 27 bar, so that the converging nozzle operates just below critical conditions. The calculations are performed with methane. The COP of the heat pump is calculated with equation 4-6.2 from Jesper et al. (2021) for standard heat pumps with hydrofluorocarbons or hydrofluoroolefins as refrigerant. The temperature of the source (ambient air) is reduced of 5 K to take into account a higher LMTD at the evaporator as the heat pumps considered in Jesper et al. are water-water heat pumps and not air-water heat pumps. The flow temperature of the heat pump is set to $T_{d,PH,ex} + 12$ K, assuming a LMTD of 10 K at the gas preheater and heat losses in the distribution loop. In summer a second scenario is considered, where the expansion turbine additionally covers the power demand of the GPRMS amounting to 5 kW_{el}. For the calculation of the electric power of the generator of the expansion turbine, the isentropic efficiency, mechanical efficiency, and generator efficiency are fixed to 0.65, 0.97, and 0.975 respectively. To calculate the primary energy savings, a gas boiler utilisation ratio of 0.85 (based on net calorific value) is considered as well as primary energy factors of 1.1 for natural gas and 1.8 for electricity. The savings are calculated for the total energy demand of the GPRMS (power and heat for gas preheating) compared to a case where the pressure reduction takes place with a conventional throttling.

Tab. 2: Calculated temperatures and performance of the expansion turbine and heat pump unit for different representative operating conditions of the year. The expansion turbine unit is designed to meet the total heat demand of the station in a typical summer day. Values marked with an asterisk (*) are measured.

Parameter	Unit	Summer (mean Jun-Aug)	Summer (mean Jun-Aug) incl. GPRMS power	Winter (mean Dec-Feb)	Autumn / spring (mean Sep-Nov & Mar-Mai)
\dot{V}_n (*)	m ³ /h	4,170	4,170	20,418	10,926
T_u (*)	°C	13.8	13.8	7.9	10.7
T_d (GOT) (*)	°C	15.7	15.7	4.8	8.1
$T_{d,PH,tot}$	°C	40.6	40.6	31.5	34.3
$T_{u,PH,ex}$	°C	21.6	21.6	11.5	14.2
$T_{d,PH,ex}$	°C	46.3	46.3	34.9	38.5
T_{amb} (*)	°C	18.3	18.3	4.0	10.0
COP	-	3.6	3.6	3.3	3.5
$\dot{V}_{n,ex}$	m ³ /h	2,214	2,842	2,214	2,214
$P_{el,ex}$	kW	25.0	32.1	24.0	24.4
\dot{Q}_{HP}	kW	89.0	96.5	80.0	85.5
\dot{Q}_{aux}	kW	0.0	0.0	220.0	86.0
$\dot{Q}_{PE,save}$ (GPRMS)	%	90.0	100.0	19.4	39.1

The results are presented in Tab. 2. At the design point in summer, 53 % of the total gas flowing through the station flows through the expansion turbine unit. The expansion turbine has an electric power of 25 kW respectively 32 kW (+28 %) if the power demand of the GPRMS is also covered. It results in primary energy savings of 90 % respectively 100 % in summer. With this dimensioning of the expansion turbine, primary energy savings of 39 % can be achieved in autumn / spring and 19 % in winter. The savings would be increased by 4, respectively 3 %-point if the power consumption of the station was additionally covered by the expansion turbine (not presented in Tab. 2). As indication, 42 % of the total annual energy demand for gas preheating took place in 2020 over the three winter months, 47 % during the six autumn / spring months and the remaining 11 % during the three summer months. The slight decrease of the expansion turbine electrical power observed in autumn / spring and winter compared to summer is caused by different gas properties due to lower gas temperatures. Interestingly the COP of the heat pump does not significantly vary along the year as the lower ambient air temperatures are compensated by lower GOT in winter and autumn / spring than in summer, due to lower water vapor dew point temperatures.

5. Conclusions and outlook

Novel concepts for the decarbonisation of gas preheating in the gas transport sector are presented in this work. Air dehumidification by a novel liquid desiccant air conditioning system could already be realized in a long-term field test and showed additional primary energy savings of 11.6 % for a year compared to a reference case without dehumidification. The solution combining an expansion turbine with heat pumps is still in the design phase, but preliminary investigations also showed a good potential for further savings. By designing the expansion turbine and heat pump unit to cover the total typical heat demand of the studied GPRMS in summer, 90 % primary energy savings can be achieved on typical summer days, 39 % in autumn / spring and 19 % in winter, considering the total energy consumption of the GPRMS (electric power and heat demand). Increasing the nominal power of the 25 kW_{el} expansion turbine by 28 % enables covering the power demand of the GPRMS, and thus allows further primary energy savings. Further investigations, including economic considerations are foreseen to compare the different configurations in more details. Whether these systems will be adopted in the future remains to be seen, depending on possible regulatory barriers and their economic viability.

6. Acknowledgments

The authors are thankful to the Federal Ministry for Economic Affairs and Climate Action (BMWK) for funding the research project ASTEREX (grant number: 03EE5101A) and to State of Hesse for funding the project LDAC-Anlage (grant number: 20005248) through the European Regional Development Fund.

7. References

- BMJV, 2021. Energiewirtschaftsgesetz vom 7. Juli 2005 (BGBl. I S. 1970, 3621), das zuletzt durch Artikel 84 des Gesetzes vom 10. August 2021 (BGBl. I S. 3436) geändert worden ist, EnWG.
- DVGW, 2015. Technische Regel – Arbeitsblatt – DVGW G 499 (A) – Erdgas-Vorwärmung in Gasanlagen. DVGW, Bonn.
- Jesper, M., Schlosser, F., Pag, F., Schmitt, B., Walmsey, T.G., Vajen, K., 2021. Large-scale heat pumps: Uptake and performance modelling of market-available devices, *Renewable and Sustainable Energy Reviews*, Volume 137, <https://doi.org/10.1016/j.rser.2020.110646>
- Louvet, Y., Ritter, D., Pag, F., Heinzen, R., Grebe, D., Vajen, K., 2021. Innovative erneuerbare Wärmeversorgungskonzepte für die Dekarbonisierung des Gastransportsektors, in: *Proceedings 31. Symposium Solarthermie und innovative Wärmesysteme*. Bad Staffelstein, Germany.
- Mischner, J., Fasold, H.-G., Heymer, J., Förster, F., Altfeld, K., Deutsch, M., 2015. *Gas2energy.net: systemplanerische Grundlagen der Gasversorgung, 2., überarbeitete und erweiterte Auflage*. ed, Edition gwf Gas, Erdgas. DIV, Deutscher Industrieverlag, München.
- Mischner, J., Köstner, R., Krause, K., 2019. Schaltungen zur Energierückgewinnung für die Gasvorwärmung in Gasdruckminderungsanlagen, *Fachberichte Neue Technologien*. gwf Gas + Energie.
- Solbraa, E., 2022. NeqSim - an open source process simulation software [WWW Document]. NeqSim. URL <https://equinor.github.io/neqsimhome/> (accessed 7.22.22).
- Wimmer, L., Ritter, D., Louvet, Y., Heinzen, R., Grebe, D., Vajen, K., Jordan, U., 2019. Monitoring of renewable process heat plants within the gas sector, in: *Proceedings of the ISES Solar World Congress 2019*. Santiago, Chile, doi:10.18086/swc.2019.12.14

List of symbols

$c_{p,m}$	mean isobaric specific heat capacity in J/kg/K
h	specific enthalpy in J/kg
p	absolute pressure in bar
p^*	critical pressure in bar
P_{el}	electric power in W
\dot{Q}	heating capacity in W
Q	heating energy in J
s	specific entropy in J/kg/K
T	temperature in °C
\dot{V}_n	gas volume flow rate at standard temperature and pressure (STP) in m ³ /s
Δh_i	specific enthalpy difference (real) in J/kg
Δh_s	specific enthalpy difference (ideal) in J/kg
$\Delta \omega$	humidity ratio difference in kg/kg
η_s	isentropic efficiency
$\mu_{JT,m}$	Joule-Thomson coefficient in K/bar
ρ_n	gas density at STP in kg/m ³
ω	humidity ratio in kg/kg

Subscripts

abs,in	absorber inlet
abs,out	absorber outlet
amb	ambient
aux	auxiliary heater
d	downstream
ds	downstream, ideal isentropic expansion
ex	expansion turbine
$goal$	ideal set point
HP	heat pump
$meas$	measurement
PE	primary energy
PH	preheating
$phys$	physical
PoH	process heat
ref	reference
reg	regenerator
$save$	saved
tot	total
u	upstream